Article

Dynamic Effects on Reaction Rates in a Michael Addition Catalyzed by Chalcone Isomerase. Beyond the Frozen Environment Approach

J. Javier Ruiz-Perni#a, In#aki Tun#o#n, Vicente Moliner, James T. Hynes, and Maite Roca

J. Am. Chem. Soc., **2008**, 130 (23), 7477-7488 • DOI: 10.1021/ja801156y • Publication Date (Web): 14 May 2008

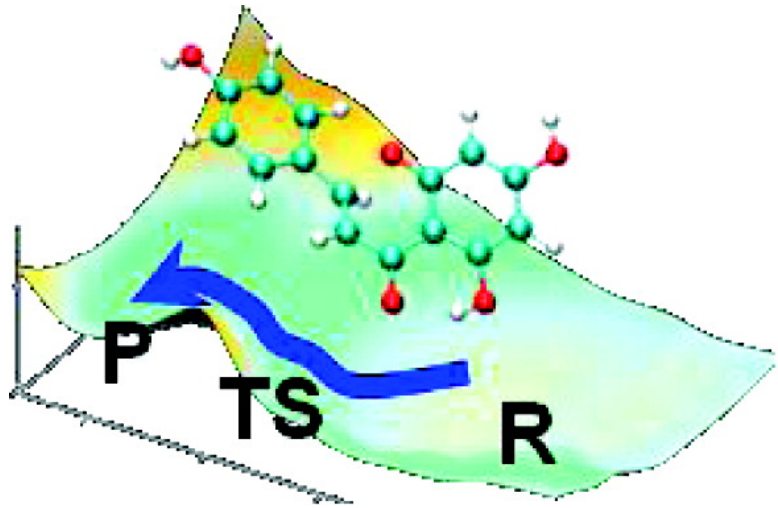

More About This Article

Additional resources and features associated with this article are available within the HTML version:

- Supporting Information
- Access to high resolution figures
- Links to articles and content related to this article
- Copyright permission to reproduce figures and/or text from this article

View the Full Text HTML

J|A|C|S
ARTICLES

Published on Web 05/14/2008

Dynamic Effects on Reaction Rates in a Michael Addition Catalyzed by Chalcone Isomerase. Beyond the Frozen Environment Approach

J. Javier Ruiz-Pernía,[†] Iñaki Tuñón,[*,†] Vicente Moliner,[*,‡] James T. Hynes,[§,||] and Maite Roca[⊥]

Departamento de Química Física, Universidad de Valencia, 46100 Burjassot, Spain, Departamento de Química Física y Analítica, Universidad Jaume I, 12071 Castellón, Spain, Département de Chimie, UMR 8640 Pasteur, Ecole Normale Supérieure, 75005 Paris, France, Department of Chemistry and Biochemistry, University of Colorado, Boulder, Colorado 80309-0215, and Department of Chemistry, University of Southern California, Los Angeles, California 90089-1062

Received February 15, 2008; E-mail: tunon@uv.es; moliner@qfa.uji.es

Abstract: We present a detailed microscopic study of the dynamics of the Michael addition reaction leading from 6′-deoxychalcone to the corresponding flavanone. The reaction dynamics are analyzed for both the uncatalyzed reaction in aqueous solution and the reaction catalyzed by *Chalcone Isomerase*. By means of rare event simulations of trajectories started at the transition state, we have computed the transmission coefficients, obtaining 0.76 ± 0.04 and 0.87 ± 0.03, in water and in the enzyme, respectively. According to these simulations, the Michael addition can be seen as a formation of a new intramolecular carbon−oxygen bond accompanied by a charge transfer essentially taking place from the nucleophilic oxygen to the carbon atom adjacent to the carbonyl group (C^{α}). As for intermolecular interactions, we find a very significant difference in the evolving solvation pattern of the nucleophilic oxygen in water and in the enzyme. While in the former medium this atom suffers an important desolvation, the enzyme provides, through variations in the distances with some residues and water molecules, an essentially constant electric field on this atom along the reaction progress. Grote−Hynes (GH) theory provides a useful framework to systematically analyze all the couplings between the reaction coordinate and the remaining degrees of freedom. This theory provides transmission coefficients in excellent agreement with the Molecular Dynamics estimations. In contrast, neither the frozen environment approach nor Kramers theory gives results of similar quality, especially in the latter case, where the transmission coefficients are severely underestimated. The (unusual) failure of the frozen environment approach signals the importance of some dynamical motions. Within the context of GH theory, analysis of the friction spectrum obtained in the enzymatic environment, together with normal-mode analysis, is used to identify those motions, of both the substrate and the environment, strongly coupled to the reaction coordinate and to classify them as dynamically active or inactive.

1. Introduction

Understanding the dynamic coupling between environment dynamics and chemical processes has been a subject of considerable research in the past several decades. Numerous efforts have been devoted to understanding the effect of solvent dynamics on a chemical reaction rate; for some examples see refs 1−12. More recently, considerable interest has been also focused on this type of analysis for enzymatic reactions.[13−28]

−Protein dynamics present an enormous complexity, displaying for example collective movements of very low frequencies and fast hydrogen vibrations with very large frequencies. Further, the impact of protein dynamics on chemical reactivity can range over quite different characters. Thus, it is well-known that many enzymatic processes are controlled by substrate binding or product release. Here, protein mobile loops can act as the active site's gates such that their motion can be the rate-determining step.[29] In other enzymes, the binding of the substrate can promote conformational changes in the enzyme that are needed to correctly place some catalytic residues.[30] Recent single-molecule experiments have shown that different conformational states of a particular enzyme can actually function as independent enzymes with noticeably different reaction rate

[†] Universidad de Valencia.
[‡] Universidad Jaume I.
[§] Ecole Normale Supérieure.
[||] University of Colorado.
[⊥] University of Southern California.

(1) Gertner, B. J.; Whitnell, R. M.; Wilson, K. R.; Hynes, J. T. *J. Am. Chem. Soc.* **1991**, *113*, 74–87.
(2) Kim, H. J.; Hynes, J. T. *J. Am. Chem. Soc.* **1992**, *114*, 10508–10528.
(3) Gertner, B. J.; Wilson, K. R.; Hynes, J. T. *J. Chem. Phys.* **1989**, *90*, 3537–3558.
(4) Tuñon, I.; Martins-Costa, M. T. C.; Millot, C.; Ruiz-López, M. F. *J. Chem. Phys.* **1997**, *106*, 3633–3642.
(5) Strnad, M.; Martins-Costa, M. T. C.; Millot, C.; Tuñón, I.; Ruiz-López, M. F.; Rivail, J. L. *J. Chem. Phys.* **1997**, *106*, 3643–3657.

constants.[31–34] In this case the dynamics associated with the interconversion among conformational states can determine the global rate constant.[35,36]

The present work is concerned solely with the *chemical*, i.e., bond-breaking and -making, activated step of the full enzymatic process, for which the dynamics of the environment can be responsible from departures from Transition State Theory, according to which the rate constant can be obtained via[9,37,38]

$$k^{\mathrm{TST}}(T) = \frac{k_{\mathrm{B}}T}{h}(C^\circ)^{1-n}\, e^{-\frac{\Delta G^{\ddagger}}{k_{\mathrm{B}}T}} \qquad (1)$$

where k_B is the Boltzmann constant, T, the temperature, h, Planck's constant, C°, the standard state concentration, and $\Delta G^{\ddagger}$, is the activation free energy, obtained under the assumption of equilibrium between the reaction coordinate and the rest of the coordinates of the system. The coupling of the reaction coordinate with the remaining coordinates is responsible for the existence of recrossings; these are, e.g., trajectories that return to the reactant state once they have crossed the transition state dividing surface toward the products valley without equilibrating in that valley. These recrossings are usually accounted for via a transmission coefficient ($\kappa(T)$) which has values lower than unity:

$$k(T) = \kappa(T)\,\frac{k_{\mathrm{B}}T}{h}(C^\circ)^{1-n}\, e^{-\frac{\Delta G^{\ddagger}}{k_{\mathrm{B}}T}} \qquad (2)$$

We have recently shown that Grote−Hynes (GH) theory,[26,27] based on the Generalized Langevin Equation,[2,39,40] gives a very accurate estimation of the transmission coefficient of enzymatic reactions for nonquantum particles. The use of this theory allows a deeper understanding and characterization of the coupling between the reaction and protein dynamics. The analysis of the friction kernel, which gives the time correlation function of the fluctuating forces acting on the reaction coordinate, provides an efficient way, in the context of GH theory, to quantify the coupling of the rest of the system in degrees of freedom with the selected reaction coordinate.[2]

In principle, one can imagine the passage of the reaction system across the dividing surface to be so fast that the remaining degrees of freedom remain essentially unaltered (rather than equilibrating) during that event. In this case, a frozen environment assumption (which is a special case of GH theory)[41] can be used to find κ[26,28] (it should be stressed that this assumption is not applied for the entire reaction path leading from reactants to products).[41] Previous comparisons of the transmission coefficient for enzymatic reactions obtained from molecular dynamics simulations (from the fraction of trajectories displaying recrossings) and using the frozen environment approach show a reasonable agreement, supporting this simple picture.[26,28] In the present work, we examine an enzymatic reaction in which this simple frozen environment description does not hold.

We here present an analysis of the coupling between reaction and protein dynamics for a reaction catalyzed by *Chalcone Isomerase* (CHI). CHI plays a central role in flavonoid biosynthetic pathways, catalyzing the transformation of chalcones, the biologically active (2*S*)-flavanones operating near the diffusion-controlled limit.[42] In physiological conditions the 2′-hydroxyl group is deprotonated, a requisite to proceed to an intramolecular Michael addition to the α,β-double bound (see Scheme 1). [42] This addition is the rate-limiting step of the process. CHI displays substrate promiscuity acting on several substrates, and

Scheme 1

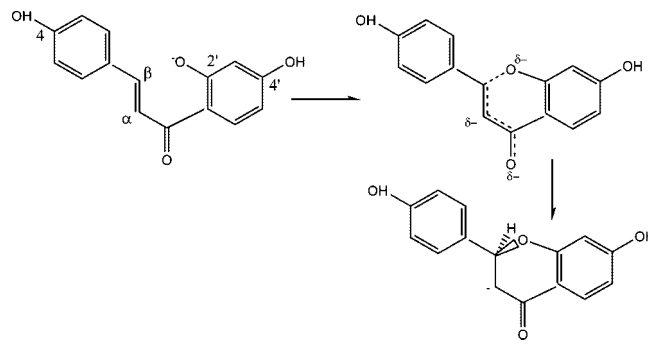

(6) Mennucci, B.; Cammi, R.; Tomasi, J. *J. Chem. Phys.* **1998**, *109*, 2798.
(7) Cramer, C. J.; Truhlar, D. G. *Chem. Rev.* **1999**, *99*, 2161–2200.
(8) Hynes, J. T. In *Solvent Effects and Chemical Reactivity*; Tapia, O., Bertrán, J., Eds.; Understanding Chemical Reactivity; Kluwer: Dordrecht, 1996; Vol. 17.
(9) Truhlar, D. G.; Garrett, B. C.; Klippenstein, S. J. *J. Phys. Chem.* **1996**, *100*, 12771–12800.
(10) Ruiz-López, M. F.; Rinaldi, D.; Bertrán, J. *J. Chem. Phys.* **1995**, *103*, 4249–9260.
(11) Geissler, P. L.; Dellago, C.; Chandler, D. *J. Phys. Chem. B* **1999**, *103*, 3706–3710.
(12) Truhlar, D. G.; Garrett, B. C. *J. Phys. Chem. B* **2000**, *104*, 1069–1072.
(13) Benkovic, S. J.; Hammes-Schiffer, S. *Science* **2003**, *301*, 1196–1202.
(14) Agarwal, P. K. *J. Am. Chem. Soc.* **2005**, *127*, 15248–15256.
(15) Kohen, A. *Prog. React. Kinet. Mech.* **2003**, *28*, 119–156.
(16) Fenimore, P. W.; Frauenfelder, H.; McMahon, B. H.; Young, R. D. *Proc. Natl Acad. Sci. U.S.A.* **2004**, *101*, 14408–14413.
(17) Olsson, M. H. M.; Parson, W. W.; Warshel, A. *Chem. Rev.* **2006**, *106*, 1737–1756.
(18) Garcia-Viloca, M.; Gao, J.; Karplus, M.; Truhlar, D. G. *Science* **2004**, *303*, 186–195.
(19) Karplus, M.; McCammon, J. A. *Annu. Rev. Biochem.* **1983**, *52*, 263–300.
(20) Neria, E.; Karplus, M. *Chem. Phys. Lett.* **1997**, *267*, 23–30.
(21) Antoniou, D.; Schwartz, S. D. *J. Phys. Chem. B* **2001**, *105*, 5553–5558.
(22) Cui, Q. A.; Karplus, M. *J. Phys. Chem. B* **2002**, *106*, 7927–7947.
(23) Basran, J.; Sutcliffe, M. J.; Scrutton, N. S. *Biochemistry* **1999**, *38*, 3218–3222.
(24) Hammes-Schiffer, S. *Biochemistry* **2002**, *41*, 13335–13343.
(25) Warshel, A.; Parson, W. W. *Science* **1989**, *246*, 112–116.
(26) Roca, M.; Moliner, V.; Tuñón, I.; Hynes, J. T. *J. Am. Chem. Soc.* **2006**, *128*, 6186–6193.
(27) Castillo, R.; Roca, M.; Soriano, A.; Moliner, V.; Tuñón, I. *J. Phys. Chem. B* **2008**, *112*, 529–534.
(28) Soriano, A.; Silla, E.; Tuñón, I.; Ruiz-López, M. F *J. Am. Chem. Soc.* **2005**, *127*, 1946–1957.
(29) Clarke, A. R.; Wigley, D. B.; Chia, W. N.; Barstow, D.; Atkinson, T.; Holbrook, J. J. *Nature* **1986**, *324*, 699–702.
(30) O'Brien, J. R.; Schuller, D. J.; Yang, V. S.; Dillard, B. D.; Lanzilotta, W. N. *Biochemistry* **2003**, *42*, 5547–5554.
(31) Kou, S. C.; Cherayil, B. J.; Min, W.; English, B. P.; Xie, X. S. *J. Phys. Chem. B* **2005**, *109*, 19068–19081.
(32) Smiley, R. D.; Hammes, G. G. *Chem. Rev.* **2006**, *106*, 3080–3094.
(33) Lu, H. P.; Xun, L. Y.; Xie, X. S. *Science* **1998**, *282*, 1877–1882.
(34) Yang, H.; Luo, G. B.; Karnchanaphanurach, P.; Louie, T. M.; Rech, I.; Cova, S.; Xun, L. Y.; Xie, X. S. *Science* **2003**, *302*, 262–266.
(35) Thorpe, I. F.; Brooks, C. L. *J. Am. Chem. Soc.* **2005**, *127*, 12997–13006.
(36) Ferrer, S.; Tuñón, I.; Marti, S.; Moliner, V.; Garcia-Viloca, M.; Gonzalez-Lafont, A.; Lluch, J. M. *J. Am. Chem. Soc.* **2006**, *128*, 16851–16863.
(37) Glasstone, S.; Laidler, K. J.; Eyring, H. *The Theory of Rate Processes*; McGraw-Hill: New York, 1941.
(38) Keck, C. J. *Adv. Chem. Phys.* **1967**, *13*, 85–121.
(39) Grote, R. F.; Hynes, J. T. *J. Chem. Phys.* **1980**, *73*, 2715–2732.
(40) Hynes, J. T. *The Theory of Chemical Reaction Dynamics*; Baer, M., Ed.; CRC Press: Boca Raton, FL, 1985.
(41) van der Zwan, G.; Hynes, J. T. *J. Chem. Phy.* **1983**, *78*, 4174–4185.
(42) Jez, J. M.; Noel, J. P. *J. Biol. Chem.* **2002**, *277*, 1361–1369.

Scheme 2

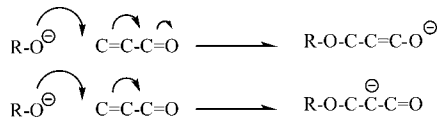

for this study we selected 4,2′,4′-trihydroxychalcone (or 6′-deoxychalcone), presented in the scheme.

As shown in our previous studies, the reaction is preceded by a conformational equilibrium between the s-cis (nonproductive) and s-trans (productive) forms of the reactant molecule due to an internal rotation around the $C^{\alpha}C(O)$ bond[43] (C(O) denotes the carbonyl carbon atom). While Michael addition is normally described as providing an enolate, our previous study of this case showed that the reaction can be better described, from the electronic point of view, as an internal charge transfer from the 2′-oxyanion to the C^{α} atom,[44] while the charge on the carbonyl oxygen did not exhibit important variations during the reaction progress (see Scheme 2).

In any event, and especially because of the important charge delocalization that can take place through the π system, the reaction should proceed with important changes in several coordinates of the system (including not only the substrate but also the interactions with the surroundings). The interest of this reaction is that, for a given distinguished reaction coordinate chosen to drive the system from reactants to products, a very important coupling with other motions of the system is expected and, as we will show below, the frozen environment approach can lead to poorer estimates of the transmission coefficient than in other cases.[23,28] This is thus an excellent example to obtain a better understanding of the coupling of the system movements to the reaction advance.

We approach this problem using several strategic components. First, we select the $O2'-C^{\beta}$ as the simplest distinguished coordinate, and using this coordinate we are able to obtain a smooth free energy profile leading from reactants to products. Next, we trace rare event reaction trajectories to compute the transmission coefficient and also to analyze the changes in the environment as the reaction proceeds. For this purpose we use a collective coordinate, an electric field, and in addition we study variations in some intra- and intermolecular coordinates of the system. Then we compute the friction kernel at the reaction transition state and use GH theory to compute transmission coefficients which are found to be in excellent agreement with the molecular dynamics estimations. Further, the analysis of the friction kernel spectra in the GH theory context allows us to know not only if there are vibrational motions strongly coupled to the reaction coordinate but also if these motions can be considered frozen or not during the barrier top passage. It is shown that there are some strongly coupled motions that are able to partially follow the system and thus are responsible for the failure of the frozen environment approach. Finally, a normal-mode analysis on a transition structure is used to identify the nature of these strongly coupled motions.

The paper is organized as follows. In the methodological section, we first give the computational details employed to carry out rare event simulations of trajectories crossing the transition state and then those related to the computation of the friction kernel to be used in GH theory. Next, the results are also given in the same order: first, we report the transmission coefficients and geometric and dynamical details obtained from reactive trajectories and, second, the application of GH theory and its combination with a normal-mode analysis carried out in the transition state.

2. Methodology

2.1. Hybrid QM/MM Model and Potentials of Mean Force. Details of the computational model are given elsewhere.[28] Briefly, we employed a hybrid quantum mechanics/molecular mechanics (QM/MM) description for our system. The reactant molecule (6′-deoxychalcone, 30 atoms) constitutes the QM subsystem, which is described using the AM1 Hamiltonian.[45] The initial coordinates of the protein were taken from the X-ray crystal structure 1EYQ.[46] Once hydrogen atoms were added, the system was placed inside a cubic box (of side 79.5 Å) of water molecules centered on the QM subsystem. The MM subsystem was then formed by 3231 enzyme atoms, 591 crystallization water atoms, and 45972 solvating water atoms, described using the OPLS-AA[47,48] and TIP3P potentials.[49] The reaction was also studied in water solvent. In this case, the simulated system was formed by the substrate, the QM part, and a cubic box (of side 55.5 Å) of TIP3P water molecules centered on the O2′ atom of the QM subsystem. For both studies of the enzymatic and solution processes, those atoms lying beyond 24 Å of the O2′ atom of the substrate were kept frozen.

The potentials of mean force (PMFs) were traced using the distance between the O2′ and the C^{β} atoms as the reaction coordinate in both media. As we have previously shown, while the use of the AM1 Hamiltonian leads to an overestimation of the free energy barrier of ~4 kcal/mol, the shape and position of the top of the barrier were in good agreement with respect to PMFs corrected using MP2/6-31+G* energies.[43,44] Since it is the latter quantities which are the important ones for the present work, we have used this hybrid AM1/MM potential in our analysis. A simplified picture of the transition state found in the active site with this methodology is presented in Scheme 3. For all the calculations, we employed a modified version of DYNAMO.[50]

As a first step in our analysis, we traced the AM1/MM PMFs in aqueous solution and in the enzyme for only a small range of reaction coordinate (RC) values (~ ±0.1 Å around the free energy maxima) using an Umbrella Potential.[51] The simulation windows are pieced together by means of the weighted histogram analysis method (WHAM).[52] These PMFs can be satisfactorily fit to a parabolic expression:

$$\Delta\mathrm{PMF} = -\frac{1}{2}K_{\mathrm{eq}}(\mathrm{RC} - \mathrm{RC}^{\ddagger})^2 \qquad (3)$$

The purpose of these PMFs being traced is to have a good estimation of the transition state position $RC^{\ddagger}$ (in terms of the $O2'C^{\beta}$ distance) and also to obtain the equilibrium barrier frequency ω_{eq} necessary for the GH analysis. This is the barrier frequency (more precisely, the absolute magnitude of the imaginary barrier fre-

(43) Ruiz-Pernia, J. J.; Silla, E.; Tuñón, I. *J. Am. Chem. Soc.* **2007**, *129*, 9117–9124.
(44) Ruiz-Pernia, J. J.; Silla, E.; Tuñón, I. *J. Phys. Chem. B* **2006**, *110*, 20686–20692.
(45) Dewar, M. J. S.; Zoebisch, E. G.; Healy, E. F.; Stewart, J. J. P. *J. Am. Chem. Soc.* **1985**, *107*, 3902–3909.
(46) Jez, J. M.; Bowman, M. E.; Dixon, R. A.; Noel, J. P. *Nat. Struct. Biol.* **2000**, *7*, 786–791.
(47) Jorgensen, W. L.; Tirado-Rives, J. *J. Am. Chem. Soc.* **1988**, *110*, 1657–1666.
(48) Kaminski, G. A.; Friesner, R. A.; Tirado-Rives, J.; Jorgensen, W. L. *J. Phys. Chem. B* **2001**, *105*, 6474–6487.
(49) Jorgensen, W. L.; Chandrasekhar, J.; Madura, J. D.; Impey, R. W.; Klein, M. L. *J. Chem. Phys.* **1983**, *79*, 926–935.
(50) Field, M. J.; Albe, M.; Bret, C.; Proust-De Martin, F.; Thomas, A. *J. Comput. Chem.* **2000**, *21*, 1088–1100.
(51) Roux, B. *Comput. Phys. Commun.* **1995**, *91*, 275–282.
(52) Torrie, G. M.; Valleau, J. P. *J. Comput. Phys.* **1977**, *23*, 187–199.

Scheme 3

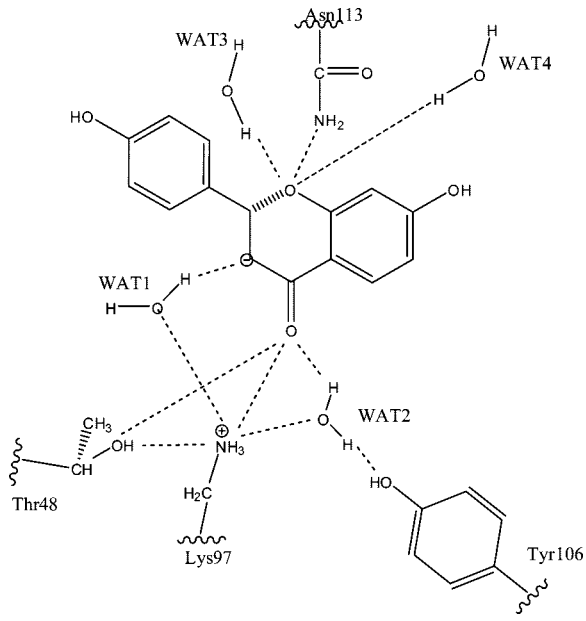

quency) under the assumption of equilibrium between the reaction coordinate and the remaining degrees of freedom (consistent with the corresponding condition for the PMFs) and is given by

$$\omega_{eq} = \frac{1}{2\pi c}\sqrt{\frac{K_{eq}}{\mu_{RC}}} \tag{4}$$

where μ_{RC} is the reaction coordinate reduced mass and c is the speed of light.

The PMFs obtained at 300 K are shown in Figure 1. To obtain these PMFs in the TS neighborhood, we ran 10 simulation windows, changing the reference value of the reaction coordinate in the Umbrella Potential by only 0.01 Å. The force constant applied to the reaction coordinate in these simulations was 2500 $kJ \cdot mol^{-1} \cdot Å^{-2}$. From the parabolic fit (with correlation coefficients ≥ 0.999), we estimate that the equilibrium barrier frequencies ω_{eq} are 800 cm^{-1} in aqueous solution and 875 cm^{-1} in the enzyme.

2.2. Rare Event Trajectories. We ran a 600 ps long NVT MD trajectory restrained in the TS region with a time step of 0.5 fs for the reaction system both in aqueous solution and in the enzyme. The simulation temperature was 300 K and one configuration was saved each 5 ps, resulting in 120 configurations that were used to compute free downhill trajectories. The velocity associated with the reaction coordinate is not properly thermalized in these configurations. Thus, following a procedure similar to that used by Gao and co-workers,[53] we selectively removed the projection of the velocity on the reaction coordinate and we added a random value taken from a Maxwell−Boltzmann distribution.

For each of the saved configurations, with modified velocities, we ran free NVE simulations integrating the equations of motion forward and backward, by just changing the sign of the velocity components.[54] Downhill trajectories were propagated from −2 ps to +2 ps using a time step of 0.5 fs. The trajectories obtained in the enzyme and in solution were then classified as reactive trajectories when reactants connect to products (RP trajectories) and nonreactive otherwise. For the latter case we found trajectories leading either from reactants to reactants (RR) or from products to products (PP). Both reactive and nonreactive trajectories may exhibit recrossings of the dividing surface. To compute the transmission

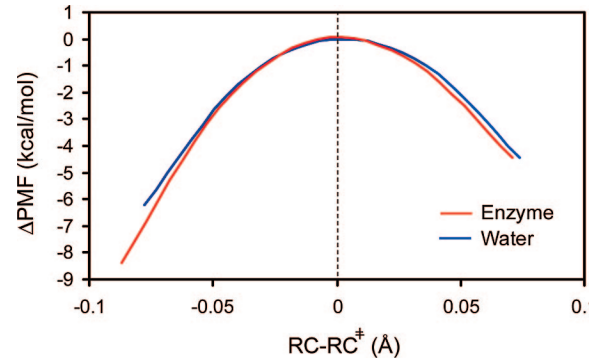

Figure 1. PMFs obtained in the vicinity of the transition state region for the reaction in water and in the CHI enzyme. Note the small range of reaction coordinate values covered and that the free energy of the transition state has been taken as zero.

coefficient we used the "positive flux" formulation,[55] assuming that the trajectory is initiated at the top of the barrier with forward momentum along the reaction coordinate. For a given time t, with $t = 0$ being the starting time for the downhill trajectory, the time-dependent transmission coefficient can be calculated as

$$\kappa(t) = \frac{\langle j_+ \theta[RC(+t)]\rangle - \langle j_+ \theta[RC(-t)]\rangle}{\langle j_+ \rangle} \tag{5}$$

where j_+ is the initial positive flux at $t = 0$ and θ(RC) is a step function equal to 1 in the product side of the reaction coordinate and equal to 0 on the reactant side. The average is calculated over all the downhill trajectories.

2.3. Application of GH Theory. GH theory can be applied to describe the evolution of the system along the reaction coordinate in the transition state. In particular, the transmission coefficient can be obtained as the ratio between the reactive frequency and the equilibrium barrier frequency ω_{eq}[3]

$$\kappa_{GH} = \frac{\omega_r}{\omega_{eq}} \tag{6}$$

with the reactive frequency ω_r obtained via the GH equation.[39,40]

$$\omega_r^2 - \omega_{eq}^2 + \omega_r \int_0^\infty \zeta_{TS}(t)\, e^{-\omega_r t}\, dt = 0 \tag{7}$$

In GH theory the friction kernel is obtained at the transition state ($\zeta_{TS}(t)$) to determine the forces exerted during the passage over the top of the barrier assuming that recrossings take place in the proximity of this dynamic bottleneck.[2,40] The analysis of the friction kernel ($\zeta(t)$), which gives the fluctuating forces acting on the reaction coordinate, provides an efficient way to quantify the coupling of the rest of the degrees of freedom of the system with the selected reaction coordinate[2]

$$\zeta(t) = \frac{\langle F_{RC}(0)\, F_{RC}(t)\rangle}{\mu_{RC} k_B T} \tag{8}$$

where $F_{RC}(t)$ is the force on the reaction coordinate, and μ_{RC}, the associated reduced mass. For the evaluation of the transition state friction kernel, we ran 100 ps of constrained MD simulations at the top of the PMF, using a Wilson's matrix-based RATTLE-like Velocity−Verlet algorithm.[56,57] A very small time step of 0.1 fs was used to ensure the convergence of the algorithm, and forces acting on the reaction coordinate were saved at each simulation step. We verified that the averaged values of the forces were close to zero in both media, ensuring that the simulations were made in

(53) Nam, K.; Prat-Resina, X.; Garcia-Viloca, M.; Devi-Kesavan, L. S.; Gao, J. L. *J. Am. Chem. Soc.* **2004**, *126*, 1369–1376.
(54) Allen, M. P.; Tildesley, D. J. *Computer Simulations of Liquids*; Clarendon: Oxford, 1989.
(55) Bergsma, J. P.; Gertner, B. J.; Wilson, K. R.; Hynes, J. T. *J. Chem. Phys.* **1987**, *86*, 1356–1376.
(56) Andersen, H. C. *J. Comput. Phys.* **1983**, *52*, 24–34.
(57) Verlet, L. *Phys. Rev.* **1967**, *159*, 98–103.

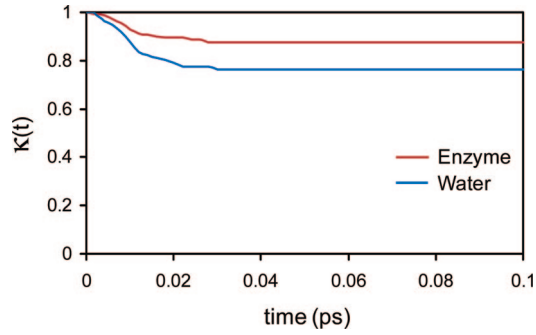

Figure 2. Time-dependent transmission coefficients obtained in the enzyme and in aqueous solution.

Table 1. Transmission Coefficients[59] Obtained from MD Trajectories, According to the Gh Theory, The Frozen Environment Limit and the Kramers Theory

	κ_{MD}	κ_{GH}	κ_{fe}	κ_{Kr}
aqueous solution	0.76 ± 0.04	0.74 ± 0.03	0.34	0.02
enzyme	0.87 ± 0.03	0.82 ± 0.02	0.56	0.03

the corresponding transition states.

As noted in the Introduction, GH theory includes as a limiting case the frozen environment approach (also called the nonadiabatic limit).[3] If the rest of the coordinates can be considered frozen compared to the motion of the reaction coordinate in the passage through the transition state, then the friction kernel can be simply replaced by its zero-time value and the reaction frequency under the frozen environment approach (ω_{fe}) is then given by

$$\omega_{fe}^2 - \omega_{eq}^2 + \zeta_{TS}(t=0) = 0 \tag{9}$$

Obviously this assumption cannot be applied to the entire reaction path.[1,24]Another interesting limit is the Kramers Theory regime[58] where it is assumed that all the friction is exerted during the barrier crossing; i.e., the time scale of the friction kernel is shorter than the inverse of ω_r.[3] In this situation, the GH equation can be rewritten as

$$\omega_{Kr}^2 - \omega_{eq}^2 + \omega_{Kr}\int_0^\infty \zeta_{TS}(t)\, dt = 0 \tag{10}$$

3. Results

3.1. Time-Dependent Transmission Coefficients. After randomizing the reaction coordinate velocity for each of the 120 saved configurations described in section 2.2, we ran free Molecular Dynamics simulations, allowing the system to evolve downhill trajectories from the transition state. Analysis of the trajectories indicated that, in the enzyme, 67 were of the RP type, 33, of the RR type, and 20, of the PP type. In solution, 54 trajectories were of the RP type, 25, of the RR type, and 41, of the PP type.

The time-dependent transmission coefficient presented in Figure 2 was evaluated using the "positive flux" formulation (eq 5). The evolution of $\kappa(t)$ shows a fast decay in both media during the first 30 fs, reaching a plateau after that. The solution and enzyme transmission coefficient values measured in this time-independent region are $\kappa_{MD,\,aq} = 0.76 \pm 0.04$ and $\kappa_{MD,\,enz} = 0.87 \pm 0.03$ (see Table 1). [59] That these values are quite close to unity indicates that Transition State Theory is a good approximation and that the selected reaction coordinate suffices to capture the essence of the changes taking place in the system

(58) Kramers, H. A. *Physica* **1940**, *7*, 284–304.
(59) For details of the error estimation procedure, see ref. 3.

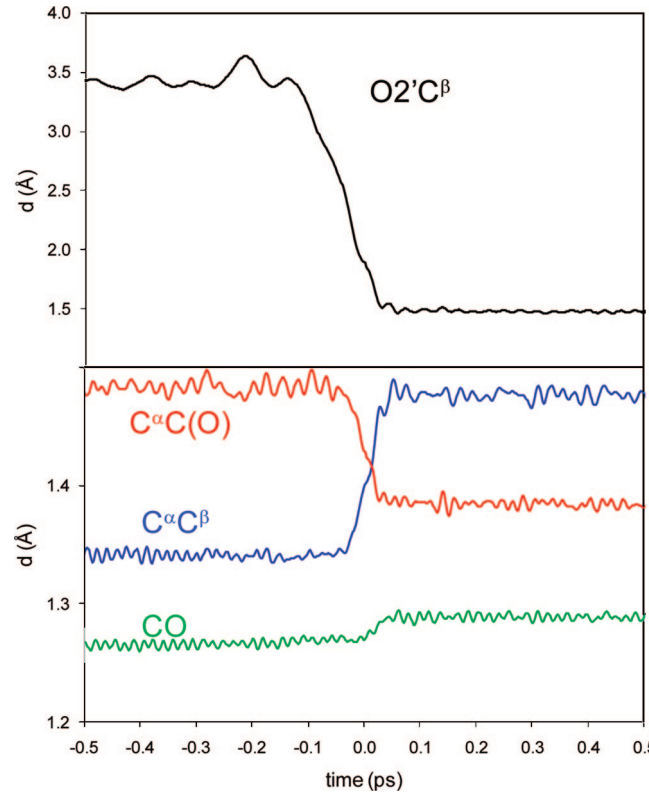

Figure 3. Time evolution of some bond distances ($O2'C^\beta$, black line; $C^\alpha C^\beta$, blue; $C^\alpha C(O)$, red; and CO, green) of the substrate along reactive trajectories in the enzyme. Only the −0.5 to +0.5 ps evolution is shown. The behavior at earlier and later times does not show any significant variation.

during the reaction. While it is noteworthy that the transmission coefficient is larger in the enzyme than in solution, its contribution to the catalytic effect ($\kappa_{enz}/\kappa_{aq} = 1.14$) is nearly negligible in view of the fact that catalysis increases the reaction rate constant by a factor of $\sim 10^5$.[42] We will return to the various theoretical estimates of the transmission coefficient after an initial discussion of the trajectory characteristics.

3.2. Analysis of Rare Event Trajectories. Detailed analysis of reactive trajectories can provide a better understanding of the chemical reaction from a microscopic point of view. Figure 3 shows the evolution of some important bond distances in the substrate for the enzymatic reaction (similar changes were observed in aqueous solution): the $O2'C^\beta$ distance (the reaction coordinate), the $C^\beta C^\alpha$ distance, the $C^\alpha C(O)$ distance, and the CO distance (the carbonyl bond length). Remember that atom labels are given in Scheme 1. The time $t = 0$ corresponds to the passage of the system over the barrier top, negative times correspond to the evolution of the system toward the reactant valley, and positive times correspond to the evolution toward the product valley. Values were averaged over the set of successful RP trajectories. It can be observed that the reaction proceeds with the formation of a new C−O bond between $O2'$ and C^β accompanied by the lengthening of the distance between the C^β and C^α atoms (which can be interpreted as the change from a double to a single bond, at least partially), the shortening of the distance between C^α and C(O) atoms (passing from a single to a partial double bond), and a slight lengthening of the carbonyl bond (corresponding to a weakening of the double bond). All these geometrical changes take place in a sequential ordering: while the change in the reaction coordinate (the $O2'C^\beta$ distance) begins at ~ -140 fs, the changes in the $C^\beta C^\alpha$, $C^\alpha C(O)$,

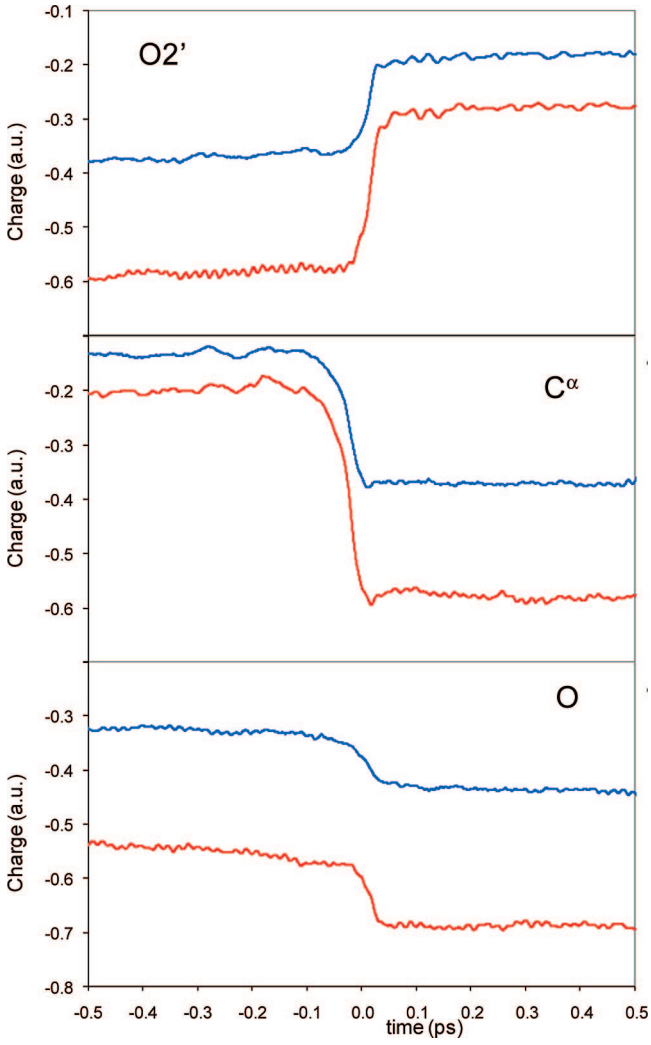

Figure 4. Time evolution of Mulliken charges averaged over reactive trajectories for some key atoms (nucleophilic oxygen O2′, C^{α} atom, and carbonyl oxygen atom O). Red line corresponds to the enzymatic reaction, and the blue one, to the reaction in aqueous solution.

and CO distances are observed at −60, −50, and −20 fs, respectively. While it is obvious from the evolution of these distances that a better reaction coordinate could be defined using an appropriate combination of them, the simple reaction coordinate that we have chosen suffices, as noted above, to provide reasonable values of the transmission coefficient.

Figure 4 shows the time evolution of the averaged Mulliken charges on some atoms of the QM subsystem: the nucleophilic oxygen atom O2′, the carbon atom C^{α}, and the carbonylic oxygen O. The Mulliken charges cannot be analyzed in absolute terms, but here we have used them in relative terms, comparing their time evolution and behavior in the different environments. As a first general feature of the three charges shown, we can see they are, in absolute magnitude, always larger in the enzyme than in solution. The larger polarization of the substrate in the active site of the enzyme compared to the water environment is a consequence of the presence of the positively charged Lys97 in the active site that, as discussed below, becomes close to the substrate as the reaction proceeds.

From the electronic point of view, the reaction can be described as a charge transfer from O2′. The charge on this atom changes from −0.6 au, in the reactant state, to −0.3 au in the product state in the enzyme and from −0.4 to −0.2 au in aqueous solution. We also observed variations in the charge on the hydroxyphenyl group attached to the C^{β} atom that changes from −0.25 au in the reactant state to −0.10 au in the product state in the enzyme and from −0.20 au to −0.05 in aqueous solution. As can be seen from Figure 4, during the Michael addition the charge is transferred essentially to C^{α}. This atom's charge changes by −0.3 au during the reaction in solution and by −0.4 au in the enzyme. The charge on the carbonylic oxygen, which is the largest charge in absolute value, does not increase in absolute magnitude as much as the charge on the carbonylic carbon atom, just by ∼0.15 au (more negative in the product state) in both environments. Thus, as found in our previous work,[43,44] the Michael addition can be viewed as a charge transfer to the C^{α} atom. While the largest absolute charge in the products is carried out by the carbonyl oxygen atom, the largest change is found on this C^{α} atom. This charge distribution will obviously assist the proton transfer to the carbon atom needed to obtain the final reaction products.

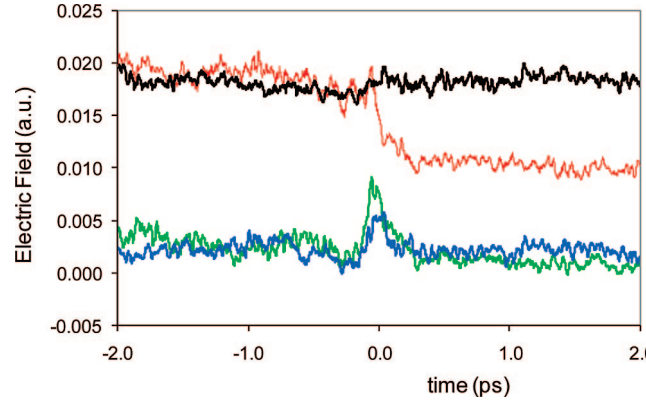

Figure 5. Electric field created by the MM environment on the O2′ atom. Black and blue lines correspond, respectively, to the modulus and the component along the O2′C^{β} direction in the enzyme. Red and green lines correspond, respectively, to the modulus and the component along the O2′C^{β} direction in the aqueous solution.

Important differences between the reactive trajectories in aqueous solution and in the enzyme appear when analyzing the behavior of the intermolecular environment. These differences can be observed using a collective coordinate, the electric field, to describe the behavior of the MM environment. This coordinate has been successfully used in other examples to understand and rationalize the behavior of the protein or the water solvent along a reaction process.[28,60] We have computed the MM contribution to the electric field on the nucleophilic oxygen (O2′) and analyzed both its modulus and component along the line connecting this atom to the attacked carbon atom (C^{β}). The results, averaged over the reactive trajectories, are shown in Figure 5.

The modulus of the electric field in Figure 5 clearly shows important differences between the behavior of the environment in water and in the enzyme. The total MM electric field felt by the nucleophilic oxygen atom clearly diminishes in water as the reaction proceeds from the reactant state to the products. This can be readily comprehended in terms of a reaction field that is much more intense when the oxygen atom has an important negative charge. Once the charge has been transferred to the rest of the system, the water molecules, surrounding the

(60) Roca, M.; Andres, J.; Moliner, V.; Tuñón, I.; Bertrán, J. *J. Am. Chem. Soc.* **2005**, *127*, 10648–10655.

O2′ atom, become much more disordered and the electric field on O2′ decreases.

In contrast to the solution situation, Figure 5 shows that in the enzyme the modulus of the electric field on the O2′ atom remains essentially invariant when the system goes from reactants to products. Certainly, this cannot be interpreted to mean that nothing is changing in the enzyme during the reaction. Indeed, as we will show below, there are changes in the environment when the reaction takes place in the active site, but these changes occur in such a way that they are able to create a constant environmental electric field on the nucleophilic O2′. In free energetic terms, this means that a free energy penalty needs to be paid for the reaction in solution since the nucleophilic O2′ must be desolvated. This is a well-known feature found in S_N2 reactions in solution.[1,28,61,62] In the enzyme, this penalty does not appear, providing one of the contributions to the free energy barrier lowering in CHI with respect to the reaction in solution.

The component of the electric field along the attacking line in Figure 5 can inform us about the electrostatic forces exerted by the MM environment against the movement of the negative charge from the O2′ to the C^{β} atom. This component is not very large. This is not unexpected because the strongest interactions with the environment are established in the direction of one of the oxygen lone pairs, so that the component along the attacking line (approximately given by the other lone pair) must be small. Further, it is interesting to note that at the crossing of the transition state, the component of the field in water is nearly twice as large as that in the enzyme. This means that in the former medium, the motion along the attacking line of the negative charge is more hindered by the MM environment than it is in the enzyme.

While the behavior of the electric field in water is well understood on the basis of a reaction field, the reasons underlying the evolution of the electric field in the enzyme remain to be clarified. For this purpose, we have analyzed the time evolution of some distances corresponding to key interactions between the substrate and the protein. As explained in our previous work on this enzyme,[43,44] in the reactant state there are two water molecules hydrogen-bonded to O2′ (Wat3 and Wat4 in Scheme 2). One of these waters (Wat4) is expelled from the active site when arriving to the transition state, while the hydrogen bond with the other water (Wat3) is shortened. This is in principle an unexpected behavior because, as analyzed above, this O2′ atom is losing negative charge (see Figure 4) so that the hydrogen bonds should be always weakened. To aid in the analysis of this issue, we have represented in Figure 6 the time evolution of this O2′−Wat3 distance averaged over the reactive trajectories, with two other averaged distances associated with important electrostatic interactions: the distance between the positively charged Lys97 with the carbonyl oxygen atom of the substrate and the distance between a water molecule (Wat1) with the C^{α} atom which receives an important fraction of the charge transferred from the nucleophilic oxygen. All the distances have been measured from the QM atom to the closest hydrogen atom of the water molecule or Lysine residue.

These three distances are now discussed, beginning with the C^{α}−Wat1 distance. The behavior of this water closer to the C^{α} atom is quite interesting because it not only provides an adequate

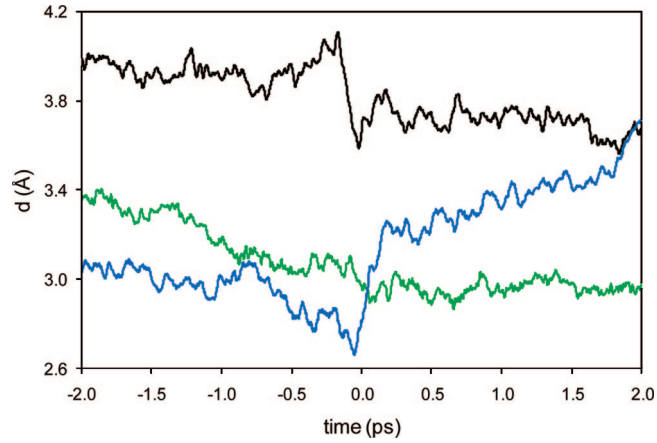

Figure 6. Time evolution of intermolecular distances averaged over reactive trajectories. The black line corresponds to the C^{α}−Wat1 distance, the green one, to the Lys97−O distance, and the blue one, to the O2′−Wat3 distance.

electrostatic stabilization of the charge transfer to this atom (this role is also played by the positively charged Lys97, see below) but also is important for the subsequent proton transfer to the carbon atom needed to reach the final products of the global reaction. While the approach of this Wat1 water to the C^{α} atom is quite modest for the substrate analyzed here (6′-deoxychalcone), we found that this effect was much stronger in the transition state of the reaction with chalcone.[43]

We next discuss the evolution of the distance between the carbonyl oxygen atom and Lys97 in Figure 6. Interestingly, this motion starts at least 2 ps in advance of the transition state crossing. Since the bond forming process just begins about 100 fs before the transition state crossing (see Figure 3), this clearly illustrates that some protein motions must precede that bond formation. This approach of the Lys97 positive charge provides an important driving force assisting the charge transfer from the O2′ atom toward C^{α} and the carbonyl oxygen atoms.

Finally, the evolution of the O2′−Wat3 distance in Figure 6 displays a minimum when the system crosses the barrier top, and thus this interaction evidently provides a transition state stabilization. As noted above, this behavior of the O2′−Wat3 interaction is counterintuitive because the negative charge is being transferred away from this oxygen as the reaction advances. This motion of the water's negative charge solvating better the nucleophilic O2′ in the transition state can be rationalized taking into account the presence of Asn113 (see Scheme 3). In some of the transition state configurations used to obtain the reactive trajectories, we found the Asn113's NH_2 group establishing a direct hydrogen bond interaction with the O2′ atom of the substrate. In other configurations, Asn113 was found at larger distances from the nucleophilic O2′, with a solvent−water molecule establishing now a hydrogen bond with this atom. In all cases, we observed a water-mediated hydrogen bond between Asn113 and Wat3. As a consequence the motions of this water molecule and Asn113 are strongly correlated as shown by Figure 7. In this figure we have plotted the evolution of the shortest O2′−Wat3 distance versus the O2′−Asn113 one averaged over the reactive trajectories. Positive and negative times are plotted separately. Both residues move simultaneously reaching a minimum distance to O2′ in the transition state. This strong correlation suggests that Asn113 can pull the Wat3 molecule toward the nucleophilic O2′ atom. The motion of Asn113 could be driven both by the displacement of the

(61) Sola, M.; Lledos, A.; Duran, M.; Bertrán, J.; Abboud, J. L. M. *J. Am. Chem. Soc.* **1991**, *113*, 2873–2879.
(62) Roca, M.; Marti, S.; Andres, J.; Moliner, V.; Tuñón, M.; Bertrán, J.; Williams, A. H. *J. Am. Chem. Soc.* **2003**, *125*, 7726–7737.

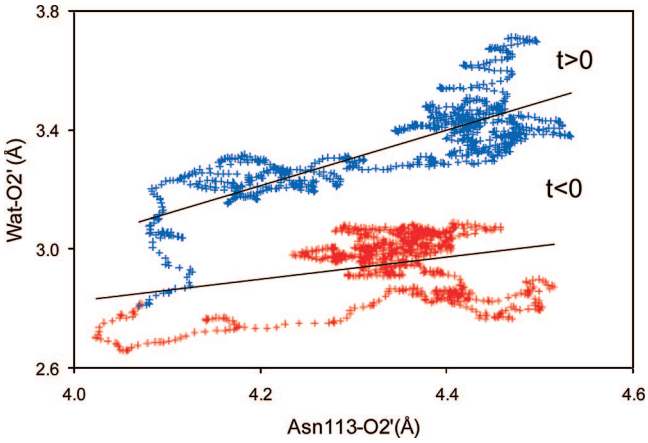

Figure 7. O2′−Wat3 distance versus O2′−Asn113 distance. These distances have been averaged over reactive trajectories. Red dots correspond to negative times (before the transition state), and blue dots correspond to positive times (after the transition state).

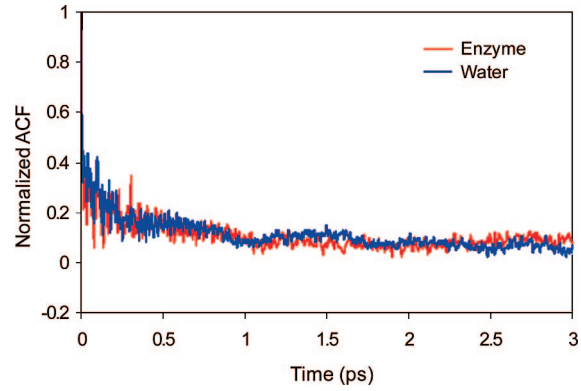

Figure 8. Normalized autocorrelation functions of the forces acting on the reaction coordinate at the transition states in water and in the enzyme.

substrate toward the Lys97—due to a stronger electrostatic interaction caused by the transfer of the charge from O2′ to groups of the substrate closer to this charged residue—and by the geometrical changes of the substrate that evolves from being planar in the reactant state to nonplanar in the transition state (the C^{β} changes its hybridization state from sp^2 to sp^3). Both these variations could distort the protein structure favoring the approach of Asn113. Thus, to sum up, one could say that the active site is fitted to accommodate the transition state, from both the geometrical and electronic perspectives.

3.3. Results of GH Theory. While the analysis of reactive trajectories can inform us about some of the details of the chemical reaction, one is clearly limited in the number of variables selected to be followed. An alternative and complementary approach is the use of the friction kernel (eq 8) in the context of GH theory as a source of information about the coupling of the reaction coordinate to all the remaining degrees of freedom. Of course, such a use should first be validated by the comparison of the transmission coefficients obtained through the use of GH theory with those already determined from MD in section 3.1.

Once the equilibrium frequency ω_{eq}, eq 4, is known, we need to evaluate the friction kernel to apply the GH eqs 6 and 7 to evaluate the transmission coefficient. The normalized version of the autocorrelation functions (ACFs) of the forces acting on the reaction coordinate at the transition state ($\langle F_{RC}(0)F_{RC}(t)\rangle_{TS}$) obtained in water and in the enzyme are represented in Figure 8. The ACFs show a remarkably similar global time evolution in both media: they decay rapidly in the first 20 fs, followed by a slow decay up to ∼1 ps. The ACFs also display a fine structure which can be attributed to the coupling of the reaction coordinate with other motions such as fast X−H stretchings, essentially the C^{β}−H stretching of the reactant molecule (this carbon atom changes from an sp^2 hybridization in the reactant state to an sp^3 in the product state as previously discussed, so an important participation of the motion of this hydrogen atom is not unexpected).

Although the time evolutions are quite similar in both environments, the zero time value of the *un-normalized* ACF eq 8 differs. The initial friction can be expressed as a wavenumber according to

$$\omega_{\zeta} = \frac{1}{2\pi c}[\zeta_{TS}(t=0)]^{1/2} \qquad (11)$$

In aqueous solution, this initial friction frequency is 755 cm^{-1}, and in the enzyme it is 725 cm^{-1}. As in other enzymatic reactions previously analyzed, the coupling between the reaction coordinate and the remainder of the system, as measured by eq 10, is stronger in solution than in the enzyme, although in the present case the difference is smaller than that found previously.[26,28] The larger value of the friction in solution with respect to the enzymatic value reflects that a larger coupling of the environment with the reaction progresses as a consequence of the changes in the charge distribution of the substrate.[26,28] As we have shown before (see Figure 5) the enzyme is able to provide a constant electric field environment, while in aqueous solution the system experiences a very different electrostatic surrounding as the reaction proceeds. The fact that the initial friction difference between the enzymatic and the solution processes is not so large in the present case can be related to the differences observed in Figure 4. Effectively, the atomic charges of the substrate change substantially more in the enzyme than in water solution. Analysis of an S_N2 reaction in solution showed that the initial friction increases with the magnitude of the solute's charge variation (a "polarization force").[3] This effect alone would increase the initial frequency in the enzyme with respect to the aqueous solution value, but nonetheless the initial friction is still slightly lower in the former environment.

With these initial friction values we can estimate the transmission coefficients under the frozen environment approach discussed in section 2.3. The values obtained using eq 9 are $\kappa_{fe,aq} = 0.34$ and $\kappa_{fe,enz} = 0.56$ (see Table 1). Interestingly both values are quite different from the MD transmission coefficients, also given in Table 1. When we computed the transmission coefficient in other examples (two S_N2 reactions catalyzed by DhlA and COMT)[26,28] the frozen environment (or nonadiabatic) approach—which as noted in section 2.2 is a limit of GH theory—gave very good transmission coefficient estimates for the enzymatic (as well as the solution) reaction, in nearly perfect agreement with MD estimations. To the best of our knowledge, this is the first reported case of an enzymatic reaction where this approach seems to fail, and thus its analysis may be very useful to gain a better understanding of the coupling between protein and reaction coordinate dynamics during the passage through the transition state dividing surface. As will be seen, the failure of the frozen environment approach can be attributed to a strong coupling with some intra- and intermolecular dynamical motions with similar or higher frequencies than the reaction frequency.

Since our subsequent analysis of the coupling will be done within the framework of GH theory, we now check if GH theory can quantitatively reproduce the MD transmission coefficients. Using eq 7, we obtained the reaction frequencies in aqueous solution and in CHI as $\omega_{r,aq} = 595\ cm^{-1}$ and $\omega_{r,enz} = 715\ cm^{-1}$. Using these frequencies and eq 6 the calculated GH transmission coefficients are $\kappa_{GH,aq} = 0.74 \pm 0.03$ and $\kappa_{GH,enz} = 0.82 \pm 0.02$.[59] The results are in perfect agreement with the MD values in Table 1, within 1 standard deviation. This encouraging result clearly shows that GH theory is applicable to enzymatic reactions even when the frozen environment approach fails. It is also noteworthy that the Kramers theory, eq 10, which considers an instantaneous system frictional response to the movement along the reaction coordinate, gives seriously underestimated transmission coefficients: 0.02 and 0.03 for the reaction in water and in the enzyme, respectively.

The large improvement obtained with GH theory as compared to its nonadiabatic limit, or frozen environment approach, is obviously due to the ability of the former to incorporate the environment's dynamics via a time-dependent friction kernel in a generalized Langevin equation. To understand in more detail the coupling between the reaction coordinate and the remaining degrees of freedom, we have analyzed this friction kernel, attempting to identify which motions participate most importantly. For this purpose, we have calculated for the solution and enzyme reactions the friction spectrum as the Fourier transform of the friction kernel.[3]

$$\zeta_{TS}(\omega) = \int_{-\infty}^{+\infty} \zeta_{TS}(t)\, e^{i\omega t}\, dt \tag{12}$$

It is more revealing to decompose the total friction spectrum into two different contributions: the relaxed spectrum ($\zeta^{+}(\omega)$) and the rigid spectrum ($\zeta^{-}(\omega)$).[3]

$$\zeta^{+}(\omega) = \frac{\zeta_{TS}(\omega)}{\omega_{eq}}\left(\frac{\omega^2}{\omega_r^2 + \omega^2}\right) \tag{13}$$

$$\zeta^{-}(\omega) = \frac{\zeta_{TS}(\omega)}{\omega_{eq}} - \zeta^{+}(\omega) \tag{14}$$

The important point is that the rigid spectrum accounts for the contributions of those motions that, while they are coupled to the reaction coordinate, can be considered as frozen during the passage over the barrier top. Then, this part of the friction is responsible for the deviations from Transition State Theory (i.e., from a transmission coefficient equal to unity) in the nonadiabatic, frozen environment limit, due to the fact that these motions remain essentially dynamically inactive during the barrier passage time scale.[3] However, the relaxed spectrum reflects those motions coupled to the reaction coordinate that can dynamically respond on the time scale of the transition state region reaction coordinate. The motions appearing in this spectrum are thus responsible for the deviations from the frozen environment limit of the transmission coefficient.[3]

The rigid and relaxed spectra, calculated from the friction kernels obtained in water and in CHI, are shown in Figure 9. The rigid spectrum in water shows more intense lines than the corresponding spectrum in the enzyme, especially below 500 cm^{-1}. This low frequency motion region corresponds in water to hindered translations, diffusion, reorientations of water molecules, and multimolecular motions, while in the enzyme this region contains assorted collective motions. The larger water spectrum intensity in this region indicates that the motions that should be considered essentially frozen are more strongly

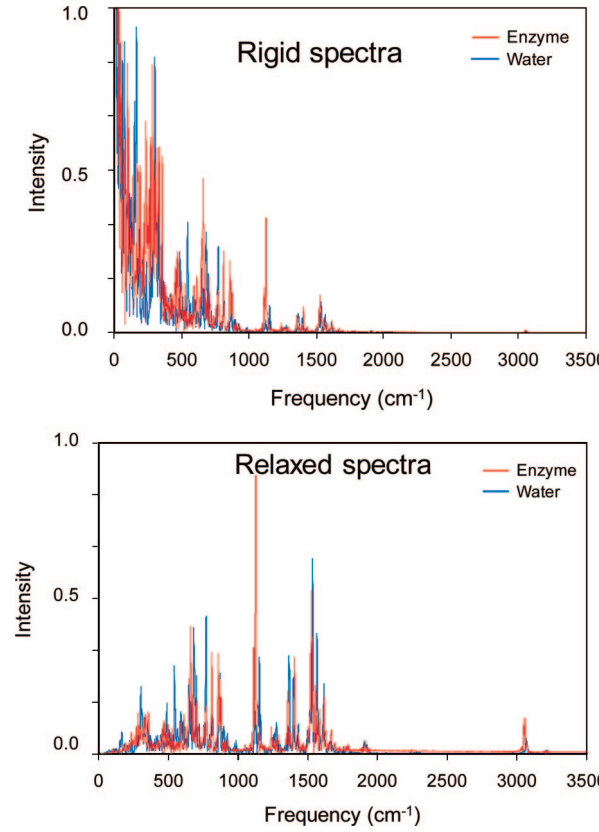

Figure 9. Rigid and relaxed friction spectra (intensity in arbitrary units) for both reaction media.

coupled to the reaction coordinate in solution than in CHI and then the frozen environment transmission coefficient estimate in solution is lower than in the enzyme. As noted above, this is related to the fact that the charge migration taking place in the substrate must be strongly sensible to the orientation of the dipole moment of the surrounding water molecules.

Turning to the relaxed friction spectra in Figure 9, the key new feature of the present reaction compared to earlier enzymatic studies[26,28] is that these spectra, responsible for the departures from the frozen environment approach, show significant strongly coupled motions not only in water but also in the enzyme. To place this in perspective, we first note that it was already known that, in aqueous solution, water librations for example can at least partially follow the barrier crossing changes in the reaction coordinate, thus contributing to an increase of the transmission coefficient with respect to the frozen environment value, [3] and such librations clearly occur in the present reaction. Moreover, X−H stretchings, usually appearing above 3000 cm^{-1}, are fast enough to be considered as fully relaxed, i.e., equilibrated during the barrier passage, and thus do not contribute significantly to the friction.[63] The novel aspect for the present reaction is the occurrence of a number of very strong lines appearing in the relaxed friction spectra in the region between 1000 and 3000 cm^{-1}, both in solution and in the enzyme. It is these motions that are largely responsible for the failure of the frozen environment estimation of the transmission coefficient.

In order to assign the important signals in the friction spectra, we have carried out a normal-mode analysis for a transition

(63) Zawadzki, A. G.; Hynes, J. T. *J. Mol. Liq.* **1991**, *48*, 197–209.

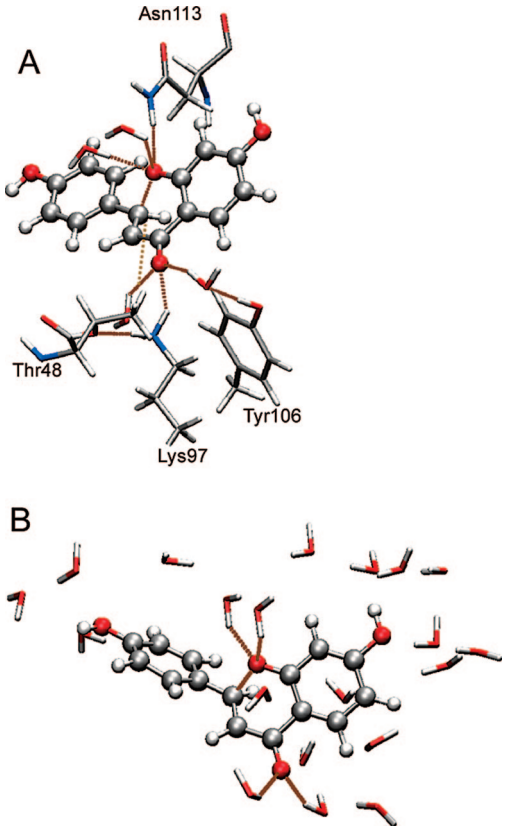

Figure 10. Transition structures for the reaction in CHI (A) and in solution (B). The pictures show only those atoms included in the control space defined to obtain the Hessian matrix.

state structure in solution and in the enzyme. The transition structures were obtained using a micro/macro iteration approach in which the coordinate's space is divided in a control space and a complementary space.[64–66] The Hessian matrix is defined only for the control space, while the complementary space is completely optimized using gradients. In the definition of the control space, we included all those residues and water molecules directly interacting with the substrate. In aqueous solution, this definition of the control space included all the coordinates of the QM subsystem (30 atoms) and 20 TIP3P water molecules (all those found at less than 3 Å from any atom of the substrate in the optimized structure), resulting in a total of 90 atoms. In the enzyme, this definition included, in addition to the substrate molecule, 4 TIP3P water molecules hydrogen bonded to O2′, the carbonyl oxygen, or the C^{β} atom and the following residues: Asn113, Thr48, part of Lys97, and part of Tyr106 (a total of 98 atoms). The transition state structures in both environments, including all the atoms of the control subspace, are shown in Figure 10.

We begin with the low frequency region of the friction spectra, defined with respect to the reaction frequencies (595 and 715 cm^{-1} in solution and in the enzyme, respectively). This region contains those coupled motions that cannot obviously respond to the changes in the reaction coordinate on the time scale of system recrossings, thus contributing to the frozen

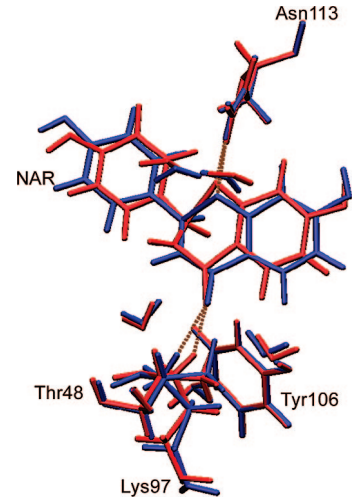

Figure 11. Representation of the high intensity motion appearing at 230 cm^{-1} in the enzymatic friction spectrum. The red and blue structures represent two snapshots of the vibration.

environment transmission coefficient. This part of the friction is highlighted in the rigid spectra. Typically this region corresponds in aqueous water to hindered translations, reorientations, and multimolecular motions of water molecules,[3] while in proteins collective motions appear in this region.[67–69] By combining the results of the normal-mode analysis with the Figure 9 friction spectra signals we have been able to identify several signals corresponding to the reorientation of the phenyl groups of the substrate coupled with motions of the surrounding water molecules or residues. These signals appear between 40 cm^{-1} and 230 cm^{-1}. In the water solution spectrum, there is a very intense signal at 165 cm^{-1} that can be described in this way. An equivalent strong signal appears in the enzymatic spectrum at 230 cm^{-1}, coupled this time to displacements of Lys97 and Asn113. The coupling of this mode, represented in Figure 11 by overlapping two snapshots of the vibrational motion, can be now related with our findings in section 3.2 concerning the displacements of Lys97, Asn113, and a water molecule (Wat3). The formation of the new $C^{\beta}O2'$ bond and the hybridization change suffered by the C^{β} carbon atom provoke a movement of the carbonyl group out of the molecular plane and modify the position of the substrate phenyl rings in the active site. These intramolecular changes are also accompanied by intermolecular changes; specifically Asn113, Lys97, and water molecules of the active site are displaced. The motion of all these residues contributes to the transition state stabilization relative to the in solution reaction, as discussed above. In particular, this normal mode leads to the reduction of the distance between the carbonyl oxygen atom of the substrate and the positively charged Lys97 as the reaction advances. Because the characteristic frequency of this vibrational mode is much lower than the reaction frequency we can consider it essentially as frozen during the barrier crossing, but as illustrated in Figure 6, it must be activated several picoseconds in advance to the passage of the system through the transition state. Thus, this is a clear example of the fact that the participation of the environment motions in the reaction coordinate can be different

(64) Moliner, V.; Turner, A. J.; Williams, I. H. *Chem. Commun.* **1997**, 1271–1272.
(65) Turner, A. J.; Moliner, V.; Williams, I. H. *Phys. Chem. Chem. Phys.* **1999**, *1*, 1323–1331.
(66) Marti, S.; Moliner, V.; Tuñón, I. *J. Chem. Theory Comput.* **2006**, *2*, 216–216.
(67) Brown, K. G.; Small, E. W.; Peticolas, W. L.; Erfurth, S. C. *Proc. Natl Acad. Sci. U.S.A.* **1972**, *69*, 1467–1469.
(68) Go, N.; Noguti, T.; Nishikawa, T. *Proc. Natl Acad. Sci. U.S.A.* **1983**, *80*, 3696–3700.
(69) Chou, K. C. *Biochem. J.* **1983**, *215*, 465–469.

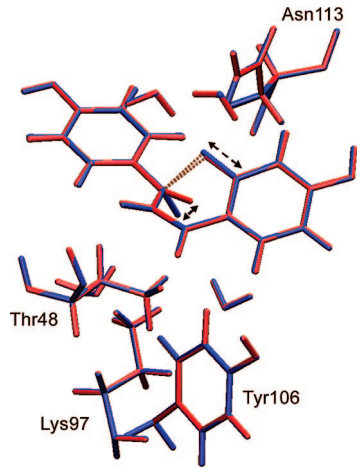

Figure 12. Representation of the high intensity motion appearing at 1130 cm^{-1} in the enzymatic friction spectrum (the corresponding signal in solution appears at 1150 cm^{-1}). The red and blue structures represent two snapshots of the vibration.

at different stages of the reaction progress. A hypothetical success of the frozen environment approach in reproducing a transmission coefficient would never imply that the environment could be viewed as static during the entire reaction process.[1]

In the region between 290 and 360 cm^{-1}, we have found several signals that can be attributed to the stretching of the hydrogen bonds established between the O2′ atom and water molecules or the carbonyl oxygen atom and water molecules. These signals appear in both media, but in the enzyme we have also found the stretching of the hydrogen bonds formed between residues Lys97 and Asn113 and the carbonylic oxygen atom and O2′ atom, respectively. The region appearing between 470 cm^{-1} and 540 cm^{-1} is dominated by librational motions of water molecules. Between 660 and 870 cm^{-1}, we have found several normal modes associated mainly with out-of-plane bending motions of the hydrogen atoms of aromatic rings (both the aromatic rings of the substrate and the aromatic ring of Tyr106 in the case of the enzyme). In the strongest signal of this region, we observed the out-of-plane motion of 6′-deoxychalcone aromatic hydrogen atoms, which is also coupled with displacements of hydrogen bonded residues Lys97 and water molecules in the enzyme and aqueous solution, respectively.

We now turn to the spectral region at higher frequencies, again combining a normal-mode analysis with the friction spectra for the mode identifications. Here the peaks correspond to motions that can, at least partially, follow the changes in the reaction coordinate in the transition state region, so that this is essentially the region responsible for the deviations from the frozen environment approach. The most intense signal in the relaxed spectrum in the enzyme appears at 1130 cm^{-1}. The same signal appears slightly displaced in water (at 1150 cm^{-1}) with a significantly lower intensity. These frequency values are significantly higher than the reaction frequencies, which were shown to be 595 and 715 cm^{-1} in solution and in the enzyme, respectively We have assigned this signal to a normal mode involving the O2′−C2′ stretching and the out-of-plane motion of the hydrogen atom bonded to the attacked carbon atom, C^{β}. Thus, this signal corresponds essentially to the change in the hybridization of this carbon, going from sp^2 to sp^3 and to the lengthening of the bond distance of the nucleophile. This mode has been represented in Figure 12 by overlapping two snapshots of the vibrational motion.

At a slightly higher frequency, at 1370 cm^{-1} both in the enzyme and in aqueous solution, appears the signal corresponding to the in-plane bending motion of the aromatic hydrogen atoms of chalcone. The signal appearing at 1400 cm^{-1} is attributed to the stretching of the aromatic carbon atoms of the substrate. The intense signals of the relaxed spectra appearing between 1530 and 1620 cm^{-1} correspond to the changes analyzed in Figure 3. The signal at 1530 cm^{-1} can be associated with the $C^{\beta}-C^{\alpha}$ stretching. The next most intense signals, appearing at 1550 cm^{-1}, essentially correspond to the $C^{\alpha}-C(O)$ stretching. Obviously, the distances associated to these bonds could be used to define a more sophisticated substrate reaction coordinate (more generally this should also include intramolecular contributions). The last important signals in this region of the spectra appear at 1620 cm^{-1} and have been assigned to the stretching of the carbonyl group of the substrate (which in the enzyme is mixed with the stretching of the carbonyl groups of the peptide bonds).

Finally, the signals appearing at about 3065 cm^{-1} correspond to the C−H stretching, mainly of the C^{α} and C^{β} atoms. In the enzyme this motion is mixed with C−H stretching of different residues (Thr48, Lys97, Tyr106, and Asn113).

As a summary of this section, the comparison of the friction spectrum and the normal-mode analysis has allowed us to identify those relevant inter- and intramolecular motions strongly coupled to the reaction coordinate. Depending on the characteristic frequencies of these motions, they can follow or not follow the changes of the reaction coordinate and they can consequently be considered as frozen or not frozen during the passage of the system over the barrier top.

4. Concluding Remarks

We have presented a detailed analysis of the reaction dynamics for the conversion of 6′-deoxychalcone into the corresponding flavanone, both in aqueous solution and in *Chalcone Isomerase*. The rate-limiting step is a unimolecular Michael addition, one of the basic reaction mechanisms in organic chemistry. To obtain a deeper insight into the dynamics of the reaction we have used a twofold strategy based, on the one hand, on the use of rare events Molecular Dynamics and, on the other hand, on the use of the Grote−Hynes (GH) theory.

Analysis of trajectories started at the transition state has allowed us not only to compute the transmission coefficient measuring the departure from Transition State Theory but also to follow some key motions of the system as the reaction evolves. Thus, the transition state stabilization provided by the enzyme has been explained in terms of key residues (Lys97 and Asn113) and water molecules present in the active site. These residues and water molecules provide an appropriate electrostatic environment for the progress of the enzyme reaction. There are important differences for the enzyme and aqueous solution reactions. In aqueous solution, the nucleophilic oxygen atom is desolvated as the reaction advances, and consequently there is a free energy penalty reflected in the larger activation free energy in solution. The use of a collective environment coordinate, here the electric field, makes more evident this differential behavior between the enzyme and the aqueous solution. On examination of the intramolecular changes taking place in the substrate (6′-deoxychlacone) we have observed important changes in the bond distances and in the electronic distribution. According to our results, the Michael addition consists of an important charge transfer to the C^{α} and, to a minor extent, to the carbonyl oxygen (see Figure 4). The

coupled geometrical changes (Figure 3) can be interpreted in terms of a mixture of two resonance forms (see Scheme 2).

GH theory has been used to provide a theoretical framework to systematically include the effect of all the degrees of freedom on the evolution of the system along the reaction coordinate in the transition state region. First, we showed that the GH theory gives the reaction transmission coefficients in excellent agreement with MD estimations, within 1 standard deviation, for both reaction media. The fact that the transmission coefficient is larger in the enzyme than in solution (which represents only a minor contribution to catalysis) can be understood considering that the effective friction on the time scale of the barrier crossing is lower in the first medium than in the second. The reason for this could be related to the fact that there is an important change in the distribution of the water solvent molecules around the nucleophilic oxygen atoms as the reaction advances and the charge, initially localized on this atom, is transferred to the C^{α} atom. This change is reflected in the evolution of the electric field on the O2′ atom during the reaction progress in aqueous solution, which shows an important desolvation effect. The same electric field computed in the active site shows no important changes during the reaction progress. It is also important to point out that this very different electrostatic behavior of the environment can be translated to an effective transition state stabilization in the enzyme's active site. Lys97 and Asn113 residues contribute to this effect.

We have also examined other approaches for the calculation of the transmission coefficients: the frozen environment approach (the nonadiabatic limit of GH theory) and the Kramers theory. The results are not as satisfactory as when using the full GH theory, especially in the latter case, which leads to a severe underestimation of the transmission coefficient (which would be translated to an important effect on the phenomenological free energy barrier). One of the distinguishing features of the reaction studied is the fact that the frozen environment approach does not work very well. The reason for this behavior is easily understood considering the important dynamical changes occurring in the remaining degrees of freedom of the system, not accounted for in the frozen environment approach. These have been analyzed by splitting the friction spectrum into a rigid spectrum, which emphasizes all those motions that can be considered essentially frozen during the reaction time scale, and the relaxed spectrum, reflecting those motions whose dynamics are important in the evolution along the reaction coordinate in the transition state region; when coupled to a normal-mode analysis, key motions can be identified. The formation of a new oxygen−carbon bond causes important changes in other bonds and degrees of freedom. First, the attacked carbon atom must change its hybridization from sp^2 to sp^3, leading to an out-of-plane motion of the bonded hydrogen atom and the lengthening of the bond to the next carbon atom. Further, other changes are observed involving this second carbon atom and the carbonyl group (which suffers from a slight lengthening of the bond distance and a displacement out of the molecular plane). The changes suffered by the substrate are also propagated to the environment resulting in the existence of enzymatic motions strongly coupled to the reaction coordinate. Thus, the hybridization change of the C^{β} atom modifies the positioning of the substrate phenyl rings, which in turns affect the distances to Asn113 and Lys97. This coupling, measured through the friction kernel spectrum, reflects the fact that a better reaction coordinate could be defined, if desired, by including more intra- and intermolecular degrees of freedom of the system and thus maximizing the transmission coefficient.[41,70,71]

Acknowledgment. We are indebted to *Ministerio Educación y Ciencia* for Project CTQ2006-15447-CO2-02 and *Generalitat Valenciana* for Projects GV06-021 and 865/2006, which supported this research. J.J.R.-P. thanks the Spanish *Ministerio de Educación y Ciencia* for an FPU doctoral fellowship. I.T. acknowledges the financial support of the Ecole Normale Supérieure (Paris) during a stay as visiting professor at ENS and the warm hospitality of the Département de Chimie. M.R. thanks Universitat Jaume I and the Generalitat Valenciana for postdoctoral fellowships. J.T.H. acknowledges the support from the CNRS and from NSF Grant CHE-0417570.

JA801156Y

(70) Gertner, B. J.; Bergsma, J. P.; Wilson, K. R.; Lee, S.; Hynes, J. T. *J. Chem. Phys.* **1987**, *86*, 1377–1386.
(71) Pu, J.; Gao, J.; Truhlar, D. G. *Chem. Rev.* **2006**, *106*, 3140–3169.